Electromagnetic Science
vol. 4, no. 1, 0130542, March 2026
https://doi.org/10.23919/emsci.2025.0054

RESEARCH ARTICLE

Observation of Fractional Disclination Charges Induced by Gain and Loss

Ruifeng Li[1,2†], Rimi Banerjee[2†], Subhaskar Mandal[3†], Da Li[1†], Yang Long[2], Tianchi Ma[1], Jian-Wei Liu[2], Gui-Geng Liu[5,6], Yidong Chong[2,4], Baile Zhang[2,4], and Er-Ping Li[1]

1. College of Information Science & Electronic Engineering, Zhejiang Key Laboratory of Intelligent Electromagnetic Control and Advanced Electronic Integration, Zhejiang University, Hangzhou 310027, China
2. *Division of Physics and Applied Physics*, *School of Physical and Mathematical Sciences*, *Nanyang Technological University*, *Singapore 639798*, *Singapore*
3. *Department of Physics*, *Indian Institute of Technology Bombay*, *Mumbai 400076*, *India*
4. *Centre for Disruptive Photonic Technologies*, *Nanyang Technological University*, *Singapore 639798*, *Singapore*
5. *Research Center for Industries of the Future*, *Westlake University*, *Hangzhou 310030*, *China*
6. *Department of Electronic and Information Engineering*, *School of Engineering*, *Westlake University*, *Hangzhou 310030*, *China*

Corresponding authors: Ruifeng Li, Email: li_ruifeng@zju.edu.cn; Yidong Chong, Email: yidong@ntu.edu.sg; Baile Zhang, Email: blzhang@ntu.edu.sg; Er-Ping Li, Email: liep@zju.edu.cn.
†Ruifeng Li, Rimi Banerjee, Subhaskar Mandal, and Da Li contributed equally to this work.
Received September 5, 2025; Accepted December 26, 2025; Published Online January 21, 2026.

Abstract — Fractional charge, a hallmark of modern electric polarization theory, provides a topological framework for understanding quantized polarization. It has only recently been recognized that real-space topological defects, such as disclinations, can further modify charge fractionalization, as an interplay between momentum-space and real-space topologies. So far, all the demonstrated mechanisms that lead to fractional disclination charges have been limited to Hermitian or energy-conserved systems. Although the non-Hermiticity has theoretically been predicted as a new route to modifying fractional disclination charge, experimental evidence remains lacking, mainly because of the challenges in measuring biorthogonal bases and precisely controlling gain/loss. Here, on a circuit metamaterial platform, we experimentally demonstrate the fractional disclination charge modification solely by manipulating the gain/loss. In experiments, negative resistors are employed as on-site gain, while positive ones as on-site loss. By measuring admittance and calculating the local density of states, we observe the topological disclination states and the associated fractionalized disclination charge. Moreover, by precisely tuning the spatial distribution of gain and loss, we observe a transition in disclination charge from fractional to integer values, which coincided with the vanishing of localized disclination states and a topological phase transition from nontrivial to trivial. Our experimental observations demonstrate a distinctive interplay between non-Hermiticity and real-space topological defects.

Keywords — Topological circuit, Metamaterial, Fractional charge, Disclination states, Gain and loss, Non-Hermitian physics.
Citation — Ruifeng Li, Rimi Banerjee, Subhaskar Mandal, *et al*., "Observation of fractional disclination charges induced by gain and loss," *Electromagnetic Science*, vol. 4, no. 1, article no. 0130542, 2026. doi: 10.23919/emsci.2025.0054.

I. Introduction

The modern electric polarization theory [1], [2] establishes a framework for quantized polarization that manifests physically as bound spectral charges. The filling anomaly of these spectral charges [3], shown as the fractional charges at domain boundaries, has stimulated research on topological states with higher codimension (such as corner states in two-dimensional (2D) [4], [5] and hinge/corner states in three-dimensional (3D) [6], [7]). However, fixed to specific values, the quantized fractional charges that are exponentially localized at corners are constrained by the band topology properties of certain 2D lattices. Until recently has it been recognized that real-space topological defects, such as dislocations and disclinations [3], [8]–[12], can further modify charge fractionalization beyond conventional momentum-space band topology [13], [14]. This interplay between momentum-space and real-space topologies has been validated in both microwave metamaterials [15] and photonic crystals [16], which facilitats the engineering of topologi-

Electromagnetic Science

cal states with geometric defects [17]–[20].

Thus far, all demonstrated mechanisms leading to fractional disclination charges have been limited to Hermitian systems (i.e., energy-conserved systems). Recently, non-Hermitian (NH) systems have attracted significant attention due to their exotic properties absent in Hermitian counterparts, such as exceptional points, NH skin effect, and non-Bloch band theory [21]–[29]. By incorporating gain and/or loss, non-Hermiticity can provide additional degrees of freedom for manipulating topological characteristics. For instance, non-Hermiticity has been utilized for inducing NH topological end states in one-dimensional (1D) lattices [30]–[33] and corner states in 2D lattices [34], [35], both associated with spectral charges. In addition, topological disclination states are identified in NH lattices [36], further providing a new route to modify fractional disclination charge. However, experimental evidence is still lacking because of technical issues. On one hand, the definition of electric polarization in Hermitian systems cannot be straightforwardly extended to NH systems, owing to the ill-defined orthogonality of eigenstates [37], [38]. On the other hand, the precise regulation of gain and loss parameters presents substantial technical difficulties [39]–[43].

Here, using a circuit metamaterial platform, we experimentally observe the fractional disclination charge sorely by manipulating the gain/loss. Due to the precise tunability of gain and loss, electrical circuits serve as a versatile platform for exploring topological NH phases [44]–[53]. In our experiments, negative resistors and conventional resistors are embedded into the circuit metamaterial to implement gain and loss on-site potentials, respectively. By combining admittance matrix measurements with mode density calculations below the Fermi level, we establish biorthogonal bases and analyze the local density of states (LDOS) distribution in our C5-symmetric circuit metamaterial. These analyses confirm the emergence of both fractionalized disclination charge (1/2 modulo 1) and topological disclination states. Moreover, by precisely tuning the spatial distribution of gain and loss, we observe a transition in disclination charge from fractional to integer values, accompanied by the vanishing of localized disclination states (leaving only a pure bandgap) and a topological phase transition from nontrivial to trivial. Monochromatic field excitation enables direct visualization of the disclination mode profile and its localization—a crucial manifestation of charge fractionalization. Furthermore, we demonstrate twofold degenerate midgap disclination states induced by gain and loss in C4-symmetric lattices. These very similar observations in both C4- and C5-symmetric systems establish general principles governing the interplay between gain-loss mechanisms and real-space disclinations.

II. Materials and Methods

1. Circuit sample construction

Circuit elements are selected and validated using the LT-spice simulation software. The NH disclination circuits are constructed using pre-selected components with the following specifications: capacitors $C_t = C_0 = 2.2$ nF (±1%), inductors $L_0 = 22$ μH (±1%), and resistors $R_0 = 154$ Ω (±5%), configured to achieve $\gamma/t = 1.3$, in which t represents the nearest hopping in circuit lattices. The INIC is implemented by utilizing the LM6171 unity-gain stable operational amplifiers (Texas Instruments). To ensure operation within the linear region of the LM6171, we select $R_a = 300$ Ω and verify stability through simulation. At the ten disclination core sites, which are characterized by reduced circuit connections, we employ capacitors with $C_0 = 4.4$ nF (±1%) to maintain the Laplacian form.

To minimize electromagnetic coupling, the printed circuit board (PCB) is designed with ground layers inserted between the source and signal layers. Signal traces are implemented with a width of 0.508 mm to minimize parasitic inductance, while power supply traces are designed to have a width of 0.635 mm to enhance their operational stability. Components are spaced at minimum intervals of 1.5 mm to reduce inductive coupling interference. The C5-symmetric PCBs comprise 15 circuit unit cells and 10 disclination sites, with a total of 280 sites across a 569 mm × 548 mm board area.

2. Experimental measurements

Admittance eigenvalues and eigenstates are characterized through scattering matrix ($\boldsymbol{S}$) measurements using a vector network analyzer (VNA) (Keysight E5061B). The operational amplifiers are powered by a DC supply providing ±15 V. The impedance matrix $\boldsymbol{Z}$ is derived using the microwave network transformation: $\boldsymbol{Z} = Z_0(\boldsymbol{I}+\boldsymbol{S})(\boldsymbol{I}-\boldsymbol{S})^{-1}$ [54], where Z_0 represents the VNA port impedance and $\boldsymbol{I}$ denotes the identity matrix. This impedance matrix $\boldsymbol{Z}$, being the inverse of the circuit Laplacian $J(\omega_0)$, provides comprehensive information about the admittance eigenvalues and eigenstates. Direct circuit site excitation measurements are also carried out using the VNA (Keysight E5061B), with subsequent vector superposition post-processing.

III. Results

1. Implementing disclination metamaterials with tuned gain-loss

As shown in Figure 1(a), by removing a $\pi/3$ sector (where the Frank angle equals $\pi/3$) from a graphene lattice and implementing a cut-and-glue procedure, we create a C5-symmetric circuit metamaterial containing a disclination at the core. After precisely tuning the on-site gain and loss distributions, we initially examine metamaterial exhibiting topologically nontrivial and trivial phases, as shown in Figures 1(b) and 1(c), respectively. The circuit metamaterial platform implements NH lattices with topological and trivial phases (as shown in Figures 1(d) and 1(e)). The circuit design utilizes C6-symmetric units (marked by solid lines) with coupling capacitors C_t, while lattice sites connect to ground through parallel inductor L_0 and capacitor C_0. To obtain the

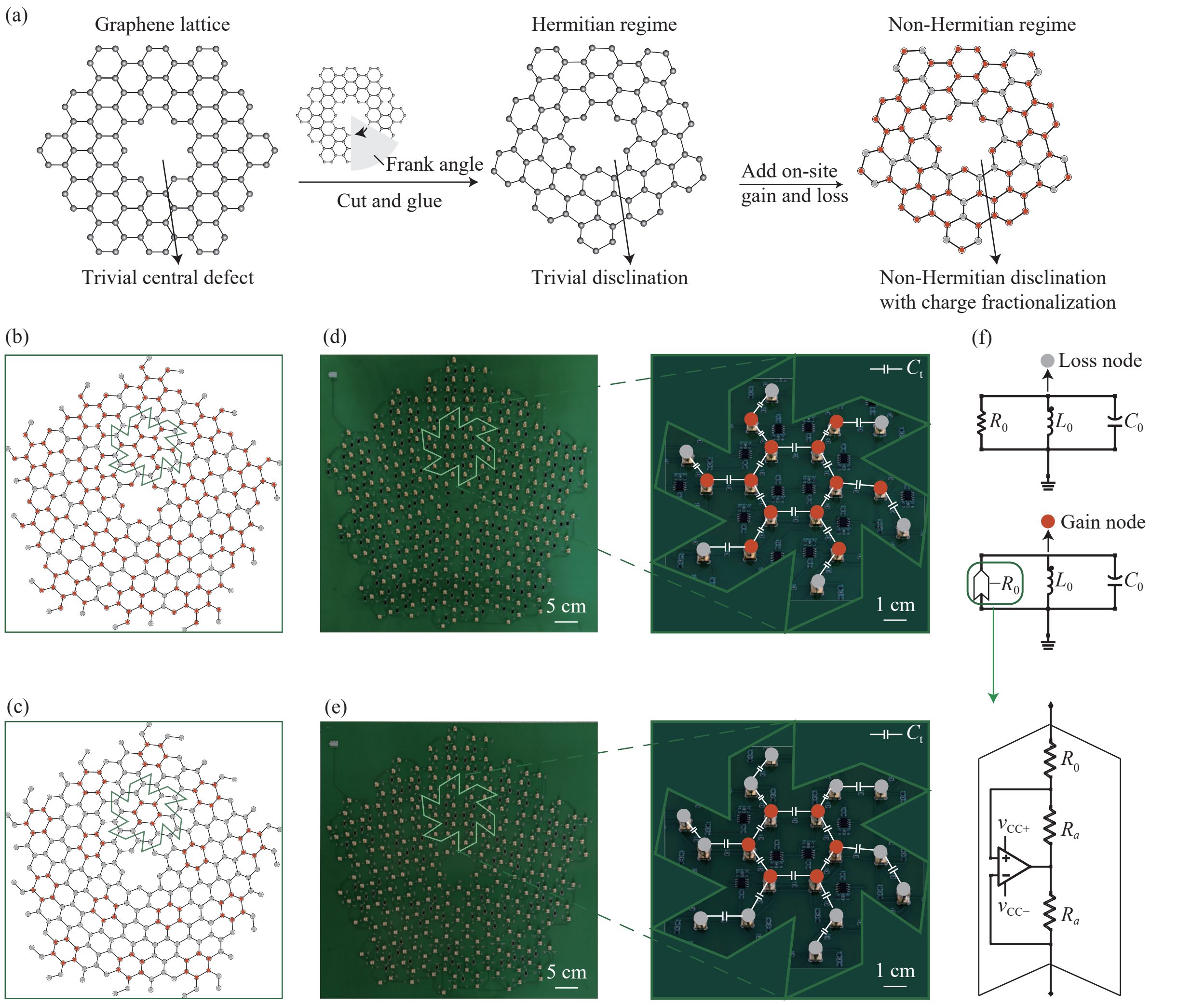

Figure 1 Circuit metamaterial and corresponding tuned gain-loss distributions. (a) Illustration of the formation of the NH disclination lattice. Schematic of NH lattices containing a disclination, with (b) Topological phase and (c) Trivial phase. Photographs of the fabricated electric circuits for C5-symmetric disclination lattices with (d) Topological phase and (e) Trivial phase. The C6-symmetric solid line box outlines a unit cell and the inset presents its enlarged view. (f) Circuit representation of the on-site potential in NH lattices. R_a denotes the balance resistor. The operational amplifiers are powered by a DC supply providing voltages v_{CC+} and v_{CC-} of ±15 V. On-site loss depends on resistors while on-site gain depends on negative resistor.

less lossy spectra, making the admittance easier to measure over the noise, gain nodes are realized using a negative impedance converter with current inversion (INIC) in parallel with L_0C_0 resonators. The detailed circuit configurations for gain/loss sites are shown in Figure 1(f).

Governed by Kirchhoff's laws, the circuit metamaterial's response is described by $\boldsymbol{I} = J\boldsymbol{V}$, where J denotes the circuit Laplacian, while $\boldsymbol{I}$ and $\boldsymbol{V}$ represent vectors of input currents and node voltages, respectively. Taking $a_n^\dagger$ and a_n as the creation and annihilation operators at site n, the circuit Laplacian J for NH lattices in Figures 1(d) and 1(e) can be expressed at a given frequency ω as follows:

$$J(\omega)\cdot \mathrm{i} = \sum_n \mathrm{i}\left(\mathrm{i}\omega(C_0+3C_t)+\frac{1}{\mathrm{i}\omega L_0}+\frac{1}{R_n}\right)a_n^\dagger a_n + \omega C_t\sum_{\langle nn'\rangle}\left(a_{n'}^\dagger a_n + \mathrm{h.c.}\right) \tag{1}$$

where h.c. stands for Hermitian conjugate, $\langle nn'\rangle$ indicates nearest neighbors, R_n is equal to R_0 for gain sites and $-R_0$ for loss sites, i denotes the imaginary unit, and the appendant term approaches zero when the frequency satisfies $\omega_0 = 1/\sqrt{L_0(C_0+3C_t)}$. See Note S1 in the Supporting Information for circuit Laplacian calculation and experimental details.

2. Charge fractionalization induced by gain and loss

To provide a concrete demonstration and anticipate our experimental findings, we first present the complex energy spectrum of the circuit metamaterials with different gain-loss distributions in Figures 2(a) and 2(b). The theoretical spectrum (Figure 2(a)) is derived through numerical evaluation of the circuit Laplacian $J(\omega_0)$ using (1), yielding the circuit lattice's eigen-admittance j. Furthermore, the experimental spectrum (Figure 2(b)) is obtained through circuit Laplacian characterization using a VNA. The methods for identifying both the bulk gap (indicated by red vertical dashes) and the occupied states are described in Note S2 in

Electromagnetic Science

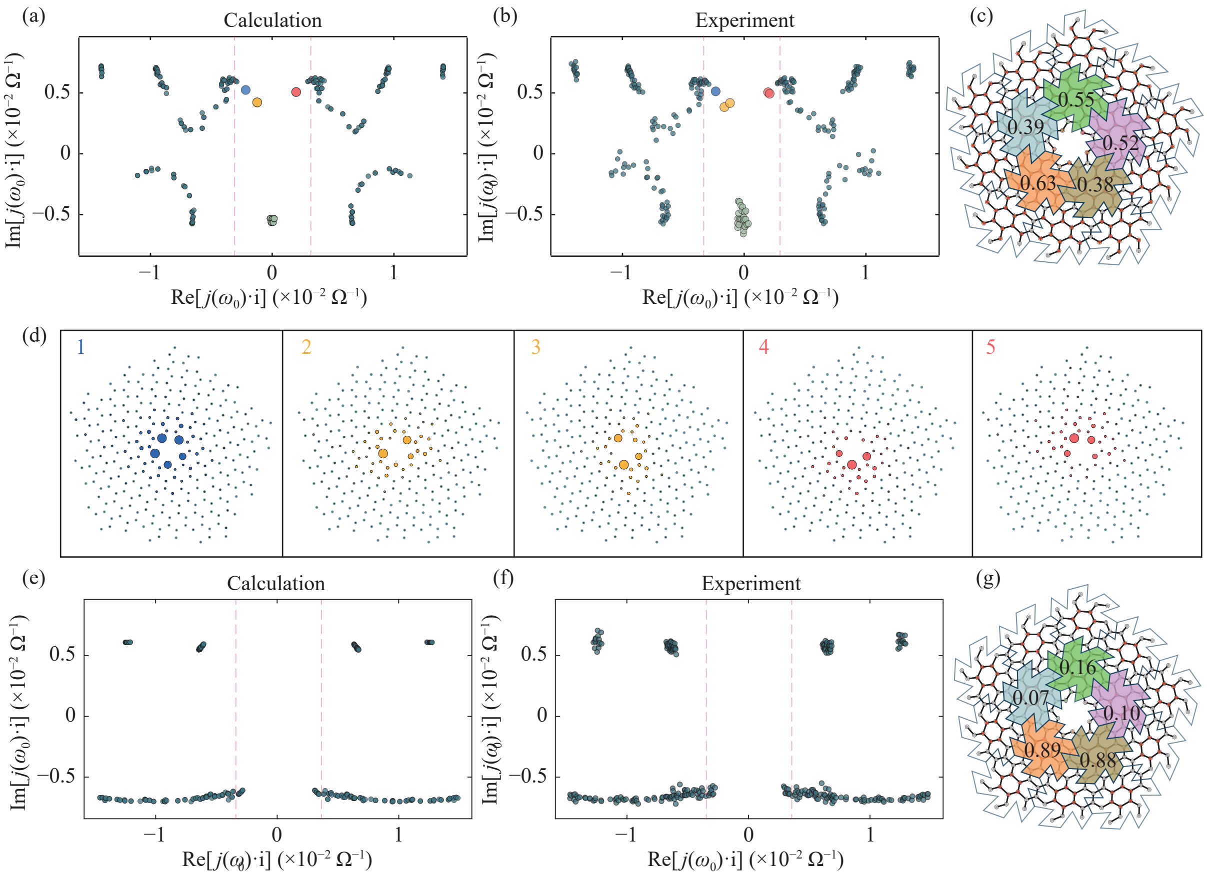

Figure 2 Fractional disclination charges induced by gain and loss in C5-symmetric electric circuit. Complex energy spectra for the NH topological circuit derived by (a) Numerical calculation and (b) Experimental measurements. The blue dot denotes the singlet mode, whereas the yellow and red dots correspond to two doublet modes. The light green clusters represent corner modes, while the dark green dots indicate edge modes and bulk states. (c) Measured spectral charge distribution in the NH topological circuit. (d) Measured voltage distributions at the resonance frequency for the five disclination states in (b). Complex energy spectra for the NH topologically-trivial circuit derived by (e) Numerical calculation and (f) Experimental measurements, showing a pure bandgap. (g) Measured spectral charge distribution in the NH topologically-trivial circuit.

the Supporting Information. Both calculation and experimental results demonstrate a good agreement in revealing five disclination states and corner modes in the mid-gap region. Moreover, Figure 2(d) illustrates experimental observations of the five localized disclination states within the bulk gap, while the phase properties are detailed in Note S3 in the Supporting Information. Following similar numerical and experimental approaches, we analyze the complex energy spectra for the topologically-trivial circuit (as shown in Figure 1(e)) with results shown in Figures 2(e) and 2(f), respectively. These spectra demonstrate a pure bandgap devoid of mid-gap states, confirming the absence of disclination modes in the trivial phase (See Note S4 in the Supporting Information for mode profiles near the bulk gap).

Next, we turn to the calculation of fractional charge of bulk unit cells near the disclination. Theoretical prediction suggests that NH disclination lattices with specific gain-loss distributions exhibit anomalous electron filling, resulting in fractional charges around disclinations [33]. Following this prediction and adopting the established methodology of analyzing LDOS in circuit metamaterials, we conduct both numerical calculations and experimental measurements on the C5-symmetric circuit in its topological phase. Following the canonical definition, the circuit disclination charge for each bulk unit cell around the disclination core can be determined as follows [33], [49], [50]:

$$Q_u = \sum_n \sum_l \left| \left\langle V_n^L | l \right\rangle \left\langle l | V_n^R \right\rangle \right| (\mathrm{mod}\ 1) \tag{2}$$

where $\langle V_n^L|$ and $|V_n^R\rangle$ represent the bi-orthogonal n-th left and right eigenvectors of the full circuit Laplacian J, which are obtained numerically from the measured circuit Laplacian. Q_u denotes the disclination charge for a bulk unit cell, with l summed over 18 sites in each bulk unit cell plus 2 nearest sites in disclination core, and n summed over all occupied states.

In our circuit metamaterial introducing gain and loss, the trapped disclination charge in each bulk unit cell clusters around 1/2 mod 1, yielding a total disclination charge of 0.47 for experiment as shown in Figure 2(c). For comparison, the respective spectral charge distributions of the circuit with trivial phase reveal charge values concentrating around 0 mod 1, with total disclination charge of 0.10 for experiment (Figure 2(g)). Those experimental results illustrate an experimental observation of charge fractionaliza-

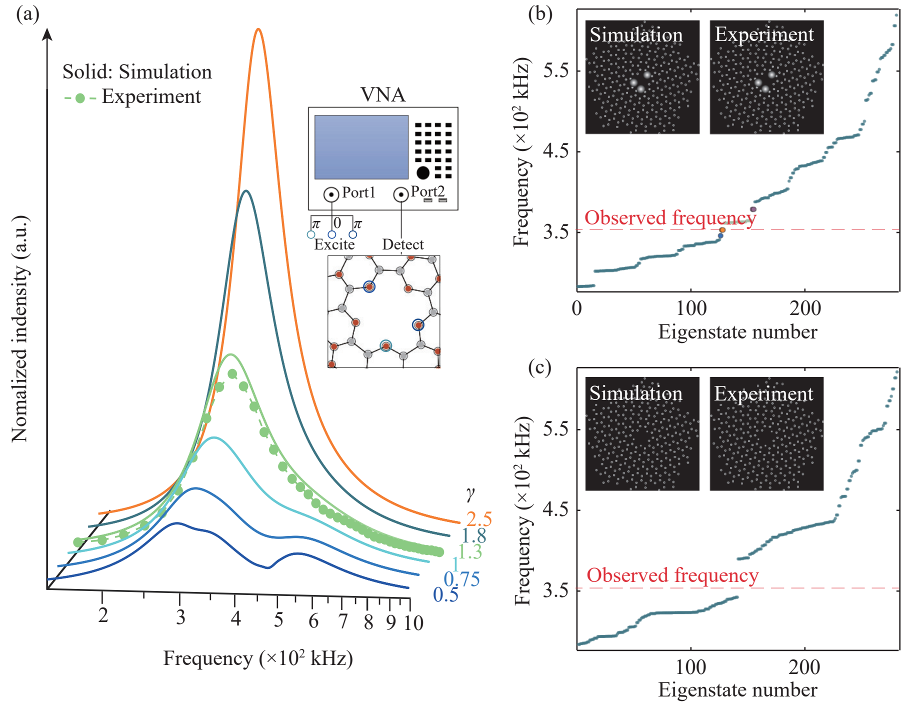

Figure 3 Direct visualization of the disclination mode profile and localization effect. (a) Frequency-dependent intensity distribution illustrating the disclination mode profile in a C5-symmetric circuit. Simulation results (solid lines) depict the behavior across varying gain/loss parameters γ (0.5–2.5), while experimental measurements (green dashed line) at $\gamma = 1.3$ are obtained using the VNA configuration shown in the inset. The eigenstate spectra of the circuit are plotted as a function of resonant frequency, comparing (b) Topological phase and (c) Trivial phase. The insets show steady-state voltage responses at the observed frequency (indicated by red dashed lines), with both simulated and experimental results displayed.

tion induced by gain and loss (see Note S5 in the Supporting Information for the Q_u calculation).

The bulk-disclination correspondence here establishes a fundamental relationship between bulk properties and charge properties localized at the disclination, given by $Q_{\text{dis}} = xq \bmod 1$, in which x is the rotational symmetry, q is the bulk Wannier center (see Note S6 in the Supporting Information for the Wannier center representation), and Q_{dis} is the disclination charge. For the topological phase, the gain-loss distribution yields $q = 0.5$, manifesting as fractional charge $Q_{\text{dis}} \approx 0.5 \bmod 1$ (Figure 2(c)). For the trivial phase, when $q = 0$, it leads to integer charge $Q_{\text{dis}} \approx 0 \bmod 1$ (Figure 2(g)). Non-Hermiticity thus enables tuning the bulk Wannier center through gain-loss distribution alone, directly controlling the disclination charge.

3. Direct visualization of the localization effect

Having observed the disclination modes and charge fractionalization phenomena through circuit Laplacian experiments, we directly visualize localization effects in the circuit metamaterial. We apply an excitation scheme based on the phase characteristics of a disclination mode from one of the doublets to investigate the localization behavior. The core intensity is quantified by calculating the sum of squared voltage amplitudes across all five disclination cores. Figure 3(a) illustrates the frequency-dependent core intensity profiles for various non-Hermiticity parameters γ (gain/loss parameters, see definition in Note S1 in the Supporting Information), implemented through adjusting the parallel resistor values R_0 in the resonators. The observed shifts in resonant frequency across different γ values show a strong agreement with theoretical predictions. The experimental measurements, indicated by green dots, are obtained through linear superposition of individual excitations at the disclination cores with precisely controlled phase differences, utilizing a VNA as shown in the inset (see detailed voltage responses in Note S7 in the Supporting Information). The experimental observation of the disclination mode shows a good agreement with simulation for $\gamma = 1.3$.

Due to the dispersive nature of circuit element admittance, observation of the circuit lattice's topological properties in the frequency domain requires the circuit Hamiltonian [51]. Figures 3(b) and 3(c) illustrate the eigenstate spectra as a function of eigenfrequency for circuits in topological and trivial phases, respectively. These frequency-domain eigenstate spectra, transformed from the measurements presented in Figures 2(b) and 2(f), preserve the topological properties of the C5-symmetric lattices. For our experimental observations, we selected the frequency $f = 353.2$ kHz corresponding to the first doublet disclination mode (indicated by horizontal red dashed lines). The circuit Hamiltonian transformation is detailed in Note S8 in the Supporting Information. The steady-state voltage responses, measured via VNA at this selected frequency, are displayed in the insets, demonstrating that the experimental measurements agree well with the numerical simulations. Notably, the topological circuit exhibits strong localization effects, manifesting as clearly observable disclination mode pro-

Electromagnetic Science

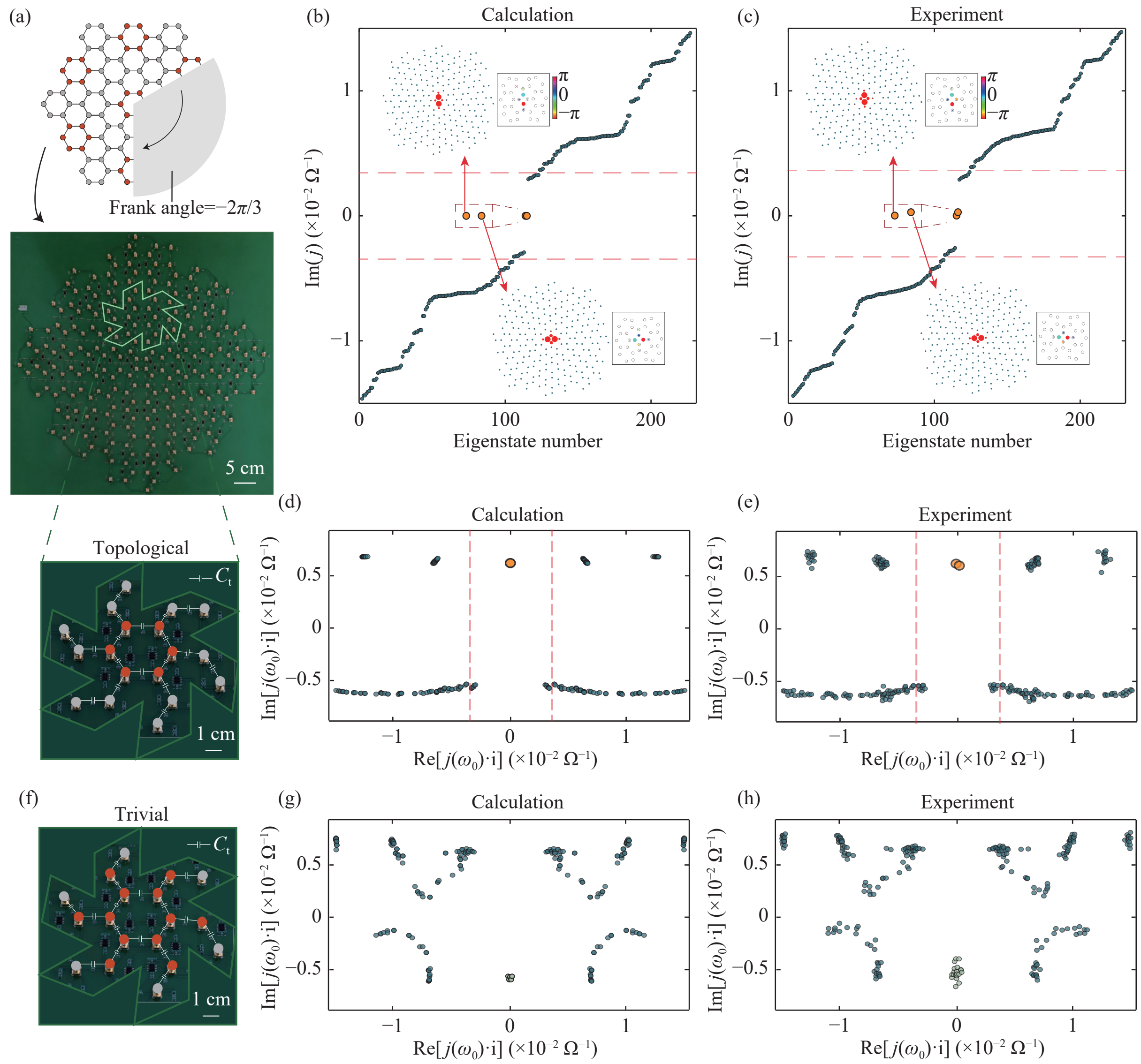

Figure 4 Degenerate zero-energy topological disclination states induced by gain and loss in C4-symmetric circuit. (a) Illustration of the C4-symmetric NH lattice formation and the photograph of the fabricated C4-symmetric NH circuit. The inset shows the enlarged view of the corresponding unit cell. Eigenstates spectra of topological circuit obtained through (b) Calculation and (c) Experiment. The inset depicts the voltage distributions of two mid-gap disclination states, including both amplitude and phase information. Complex energy spectra derived from (d) Calculation and (e) Experiment. (F) Photograph of the fabricated C4-symmetric NH circuit unit cell with an alternative gain/loss configuration. Complex energy spectra obtained through (g) Calculation and (h) Experiment.

files at the observation frequency, as shown in Figure 3(b). In contrast, the trivial circuit configuration (Figure 3(c)) displays no such localization, because the observation frequency lies within a spectral gap where mode excitation is suppressed.

4. Degenerate zero-energy topological disclination states induced by gain and loss

We further expanded our investigation to include a C4-symmetric circuit configuration by removing a $2\pi/3$ sector from the honeycomb lattice with different gain-loss distributions, as illustrated in Figure 4(a). Figure 4(a) presents the fabricated C4-symmetric circuit metamaterial, with the inset providing a detailed view of the unit cell structure. The eigenstate spectra, derived from both theoretical calculations (Figure 4(b)) and experimental measurements (Figure 4(c)), reveal distinct degenerate mid-gap states, serving as a gain-loss analogue to the results reported by Deng *et al.* [55]. The insets display the voltage distribution patterns of these disclination states, encompassing both amplitude and phase information. The twofold degeneracy of the midgap disclination modes in the C4-symmetric lattice is a consequence of the C4 rotational symmetry. Unlike C5, which only has 1D irreducible representations, the C4 point group possesses a 2D irreducible representation. The disclination states belong to this representation and must appear as a degenerate pair to preserve the C4 symmetry, as both states are required to form a complete basis under rotation.

Furthermore, the corresponding complex energy spectra obtained from theoretical calculations (Figure 4(d)) and

Electromagnetic Science

experimental measurements (Figure 4(e)) demonstrate a good agreement, clearly indicating the emergence of zero-energy topological disclination states. In contrast, the C4-symmetric NH circuit metamaterial with transitioned gain/loss pattern (Figure 4(f)) exhibits substantially different characteristics. The complex energy spectra obtained from calculations (Figure 4(g)) and experiments (Figure 4(h)) confirm the absence of disclination states. The details about C4-symmetric circuits can be found in Note S9 in the Supporting Information.

IV. Conclusion

To summarize, we experimentally demonstrated the modification of fractional disclination charges induced sorely by gain and loss, representing a significant advancement in understanding the interplay between non-Hermiticity and real-space topology. Through admittance measurements and LDOS calculations in our circuit metamaterial platform, we observed fractional charges of approximately 1/2 (modulo 1) at disclination cores in the topological phase, which transitioned to integer values in the trivial phase. This transition coincided with the disappearance of localized disclination states, demonstrating direct evidence of engineering fractional disclination charges via gain and loss distributions. Moreover, our observations of similar phenomena in both C5- and C4-symmetric lattices establish general principles for NH charge fractionalization across different geometric configurations. The ability to control topological properties through gain and loss distribution offers a versatile approach for designing topological devices with tunable characteristics. While our current implementation focuses on the linear regime, extending this framework to incorporate nonlinear effects could lead to the development of active topological devices with adaptive responses, including topological lasers with enhanced stability properties.

Acknowledgements

The work was supported by the National Natural Science Foundation of China (Grant Nos. 62071424, 62201499, and 62027805), the Research Center for Industries of the Future (RCIF) at Westlake University (Grant No. 210000006022 312), and the Westlake Education Foundation (Grant No. 103110736022301). Yang Long gratefully acknowledged the support of the Eric and Wendy Schmidt AI in Science Postdoctoral Fellowship, a Schmidt Futures program.

Supporting Information

Supplementary Notes S1–S9. The supporting information is available online at www.emscience.org. The supporting materials are published as submitted, without typesetting or editing. The responsibility for scientific accuracy and content remains entirely with the authors.

References

[1] N. Marzari, A. A. Mostofi, J. R. Yates, *et al*., "Maximally localized Wannier functions: Theory and applications," *Reviews of Modern Physics*, vol. 84, no. 4, pp. 1419–1475, 2012.

[2] R. Resta, "Macroscopic polarization in crystalline dielectrics: The geometric phase approach," *Reviews of Modern Physics*, vol. 66, no. 3, pp. 899–915, 1994.

[3] W. A. Benalcazar, T. H. Li, and T. L. Hughes, "Quantization of fractional corner charge in C_n-symmetric higher-order topological crystalline insulators," *Physical Review B*, vol. 99, no. 24, article no. 245151, 2019.

[4] W. A. Benalcazar, B. A. Bernevig, and T. L. Hughes, "Quantized electric multipole insulators," *Science*, vol. 357, no. 6346, pp. 61–66, 2017.

[5] J. Langbehn, Y. Peng, L. Trifunovic, *et al*., "Reflection-symmetric second-order topological insulators and superconductors," *Physical Review Letters*, vol. 119, no. 24, article no. 246401, 2017.

[6] M. Ezawa, "Higher-order topological insulators and semimetals on the breathing Kagome and pyrochlore lattices," *Physical Review Letters*, vol. 120, no. 2, article no. 026801, 2018.

[7] F. Schindler, A. M. Cook, M. G. Vergniory, *et al*., "Higher-order topological insulators," *Science Advances*, vol. 4, no. 6, article no. eaat0346, 2018.

[8] T. H. Li, P. H. Zhu, W. A. Benalcazar, *et al*., "Fractional disclination charge in two-dimensional C_n-symmetric topological crystalline insulators," *Physical Review B*, vol. 101, no. 11, article no. 115115, 2020.

[9] G. van Miert and C. Ortix, "Dislocation charges reveal two-dimensional topological crystalline invariants," *Physical Review B*, vol. 97, no. 20, article no. 201111, 2018.

[10] V. Juričić, A. Mesaros, R. J. Slager, *et al*., "Universal probes of two-dimensional topological insulators: Dislocation and π flux," *Physical Review Letters*, vol. 108, no. 10, article no. 106403, 2012.

[11] R. J. Slager, "The translational side of topological band insulators," *Journal of Physics and Chemistry of Solids*, vol. 128, pp. 24–38, 2019.

[12] F. F. Li, H. X. Wang, Z. Xiong, *et al*., "Topological light-trapping on a dislocation," *Nature Communications*, vol. 9, no. 1, article no. 2462, 2018.

[13] C. W. Peterson, T. H. Li, W. A. Benalcazar, *et al*., "A fractional corner anomaly reveals higher-order topology," *Science*, vol. 368, no. 6495, pp. 1114–1118, 2020.

[14] Z. K. Lin, Y. Wu, B. Jiang, *et al*., "Topological Wannier cycles induced by sub-unit-cell artificial gauge flux in a sonic crystal," *Nature Materials*, vol. 21, no. 4, pp. 430–437, 2022.

[15] C. W. Peterson, T. H. Li, W. T. Jiang, *et al*., "Trapped fractional charges at bulk defects in topological insulators," *Nature*, vol. 589, no. 7842, pp. 376–380, 2021.

[16] Y. Liu, S. Leung, F. F. Li, *et al*., "Bulk–disclination correspondence in topological crystalline insulators," *Nature*, vol. 589, no. 7842, pp. 381–385, 2021.

[17] B. Q. Ren, A. A. Arkhipova, Y. Q. Zhang, *et al*., "Observation of nonlinear disclination states," *Light: Science & Applications*, vol. 12, no. 1, article no. 194, 2023.

[18] Z. C. Hu, D. Bongiovanni, Z. T. Wang, *et al*., "Topological orbital angular momentum extraction and twofold protection of vortex transport," *Nature Photonics*, vol. 19, no. 2, pp. 162–169, 2025.

[19] M. S. Hwang, H. R. Kim, J. Kim, *et al*., "Vortex nanolaser based on a photonic disclination cavity," *Nature Photonics*, vol. 18, no. 3, pp. 286–293, 2024.

[20] H. Y. Qin, Z. Zhang, Q. L. Chen, *et al*., "Disclination states in nonreciprocal topological networks," *Physical Review Research*, vol. 6, no. 1, article no. 013031, 2024.

[21] L. Feng, R. El-Ganainy, and L. Ge, "Non-Hermitian photonics based on parity–time symmetry," *Nature Photonics*, vol. 11, no. 12, pp. 752–762, 2017.

[22] H. T. Shen, B. Zhen, and L. Fu, "Topological band theory for non-Hermitian Hamiltonians," *Physical Review Letters*, vol. 120, no. 14, article no. 146402, 2018.

[23] Z. P. Gong, Y. Ashida, K. Kawabata, *et al*., "Topological phases of non-Hermitian systems," *Physical Review X*, vol. 8, no. 3, article

no. 031079, 2018.

[24] K. Kawabata, K. Shiozaki, M. Ueda, *et al*., "Symmetry and topology in non-Hermitian physics," *Physical Review X*, vol. 9, no. 4, article no. 041015, 2019.

[25] Y. Zhang, Z. Z. Guo, B. K. Xu, *et al*., "Performance analysis of non-paraxial deployments continuous aperture MIMO for electromagnetic information theory, " *Electromagnetic Science*, in press, 2025.

[26] P. St-Jean, V. Goblot, E. Galopin, *et al*., "Lasing in topological edge states of a one-dimensional lattice," *Nature Photonics*, vol. 11, no. 10, pp. 651–656, 2017.

[27] M. Parto, S. Wittek, H. Hodaei, *et al*., "Edge-mode lasing in 1D topological active arrays," *Physical Review Letters*, vol. 120, no. 11, article no. 113901, 2018.

[28] A. Saleem and S. R. Tan, "Modeling of intelligent reflecting surface based 3-D non-stationary massive MIMO channel for vehicle-to-vehicle communications," *Electromagnetic Science*, vol. 3, no. 4, article no. 0120382, 2025.

[29] R. F. Li, J. Y. Ma, D. Li, *et al*., "Non-invasive self-adaptive information states' acquisition inside dynamic scattering spaces," *Research*, vol. 7, article no. 0375, 2024.

[30] K. Takata and M. Notomi, "Photonic topological insulating phase induced solely by gain and loss," *Physical Review Letters*, vol. 121, no. 21, article no. 213902, 2018.

[31] H. Gao, H. R. Xue, Q. Wang, *et al*., "Observation of topological edge states induced solely by non-Hermiticity in an acoustic crystal," *Physical Review B*, vol. 101, no. 18, article no. 180303, 2020.

[32] S. Liu, S. J. Ma, C. Yang, *et al*., "Gain- and loss-induced topological insulating phase in a non-Hermitian electrical circuit," *Physical Review Applied*, vol. 13, no. 1, article no. 014047, 2020.

[33] P. Comaron, V. Shahnazaryan, W. Brzezicki, *et al*., "Non-Hermitian topological end-mode lasing in polariton systems," *Physical Review Research*, vol. 2, no. 2, article no. 022051, 2020.

[34] X. W. Luo and C. W. Zhang, "Higher-order topological corner states induced by gain and loss," *Physical Review Letters*, vol. 123, no. 7, article no. 073601, 2019.

[35] H. Gao, H. R. Xue, Z. M. Gu, *et al*., "Non-Hermitian route to higher-order topology in an acoustic crystal," *Nature Communications*, vol. 12, no. 1, article no. 1888, 2021.

[36] R. Banerjee, S. Mandal, Y. Y. Terh, *et al*., "Topological disclination states and charge fractionalization in a non-Hermitian lattice," *Physical Review Letters*, vol. 133, no. 23, article no. 233804, 2024.

[37] C. Ortega-Taberner, L. Rødland, and M. Hermanns, "Polarization and entanglement spectrum in non-Hermitian systems," *Physical Review B*, vol. 105, no. 7, article no. 075103, 2022.

[38] J. B. Hu, C. A. Perroni, G. De Filippis, *et al*., "Electric polarization and its quantization in one-dimensional non-Hermitian chains," *Physical Review B*, vol. 107, no. 12, article no. L121101, 2023.

[39] T. E. Lee, "Anomalous edge state in a non-Hermitian lattice," *Physical Review Letters*, vol. 116, no. 13, article no. 133903, 2016.

[40] K. Kawabata, K. Shiozaki, and M. Ueda, "Anomalous helical edge states in a non-Hermitian Chern insulator," *Physical Review B*, vol. 98, no. 16, article no. 165148, 2018.

[41] D. Leykam, K. Y. Bliokh, C. L. Huang, *et al*., "Edge modes, degeneracies, and topological numbers in non-Hermitian systems," *Physical Review Letters*, vol. 118, no. 4, article no. 040401, 2017.

[42] S. Weimann, M. Kremer, Y. Plotnik, *et al*., "Topologically protected bound states in photonic parity–time-symmetric crystals," *Nature Materials*, vol. 16, no. 4, pp. 433–438, 2017.

[43] M. Ornigotti and A. Szameit, "Quasi PT-symmetry in passive photonic lattices," *Journal of Optics*, vol. 16, no. 6, article no. 065501, 2014.

[44] W. X. Zhang, D. Y. Zou, Q. S. Pei, *et al*., "Experimental observation of higher-order topological Anderson insulators," *Physical Review Letters*, vol. 126, no. 14, article no. 146802, 2021.

[45] T. Helbig, T. Hofmann, S. Imhof, *et al*., "Generalized bulk–boundary correspondence in non-Hermitian topolectrical circuits," *Nature Physics*, vol. 16, no. 7, pp. 747–750, 2020.

[46] X. X. Zhang and M. Franz, "Non-Hermitian exceptional Landau quantization in electric circuits," *Physical Review Letters*, vol. 124, no. 4, article no. 046401, 2020.

[47] S. Liu, R. W. Shao, S. J. Ma, *et al*., "Non-Hermitian skin effect in a non-Hermitian electrical circuit," *Research*, vol. 2021, article no. 5608038, 2021.

[48] X. W. Zhang, C. H. Wu, M. Yan, *et al*., "Observation of continuum Landau modes in non-Hermitian electric circuits," *Nature Communications*, vol. 15, no. 1, article no. 1798, 2024.

[49] D. Y. Zou, T. Chen, W. J. He, *et al*., "Observation of hybrid higher-order skin-topological effect in non-Hermitian topolectrical circuits," *Nature Communications*, vol. 12, no. 1, article no. 7201, 2021.

[50] C. H. Lee, S. Imhof, C. Berger, *et al*., "Topolectrical circuits," *Communications Physics*, vol. 1, article no. 39, 2018.

[51] A. Stegmaier, S. Imhof, T. Helbig, *et al*., "Topological defect engineering and PT symmetry in non-Hermitian electrical circuits," *Physical Review Letters*, vol. 126, no. 21, article no. 215302, 2021.

[52] D. G. Wu, J. S. Chen, W. Su, *et al*., "Effective impurity behavior emergent from non-Hermitian proximity effect," *Communications Physics*, vol. 6, article no. 160, 2023.

[53] M. Ezawa, "Non-Hermitian higher-order topological states in nonreciprocal and reciprocal systems with their electric-circuit realization," *Physical Review B*, vol. 99, no. 20, article no. 201411, 2019.

[54] D. M. Pozar, *Microwave Engineering*, 4th ed., John Wiley & Sons, Hoboken, 2011.

[55] Y. C. Deng, W. A. Benalcazar, Z. G. Chen, *et al*., "Observation of degenerate zero-energy topological states at disclinations in an acoustic lattice," *Physical Review Letters*, vol. 128, no. 17, article no. 174301, 2022.

Ruifeng Li received the B.S. degree in electronic information engineering from University of Electronic Science and Technology of China, Chengdu, China, in 2020 and the Ph.D. degree from Zhejiang University, Hangzhou, China, in 2025. He is currently working with the College of Information Science & Electronic Engineering, Zhejiang University, Hangzhou, China. His research interests include information theory, non-Hermitian physics, and topological photonics.
(Email: li_ruifeng@zju.edu.cn)

Rimi Banerjee received the Ph.D. degree from Nanyang Technological University, Singapore, in 2025. She is currently working with Nanyang Technological University, Singapore, as a Research Fellow. Her research interests include topological photonics, terahertz 6G communication, and non-Hermitian physics.
(Email: rimi.banerjee@ntu.edu.sg)

Subhaskar Mandal joined Nanyang Technological University, Singapore, in 2021, as a Research Fellow. He is currently working with Indian Institute of Technology Bombay, Mumbai, India, as an Assistant Professor. His research interest mainly focuses on exploring novel physical phenomena in topological photonics, exciton–polaritons, and topological lasers.
(Email: subhaskar@iitb.ac.in)

Da Li received the B.S. and the Ph.D. degrees in electrical engineering from Zhejiang University, Hangzhou, China, in 2014 and 2019, respectively. From 2017 to 2018, he worked at Nanyang Technological University, Singapore, as a Project Researcher. From 2019 to 2021, he joined Science and Technology on Antenna and Microwave Laboratory, Nanjing, China, as a Research Fellow. He is currently an Assistant Professor at Zhejiang University, Hangzhou, China. His research interests include machine learning, antennas, matesurfaces, and electromagnetic compatibility. Dr. Li has authored or coauthored more than 40 refereed papers and served as Reviewers for 6 technical journals and TPC Members of 3 IEEE conferences. He was also a recipient of the Outstanding Young Scientist Award at 2022 Asia-Pacific International Symposium on Electromagnetic Compatibility.
(Email: li-da@zju.edu.cn)

Yang Long received the Ph.D. degree from Tongji University, Shanghai, China, in 2020. From 2021 to 2025, he served as a Research Fellow at Nanyang Technological University (NTU), Singapore. In 2025, he joined the College of Physics and Electronic Engineering, Tongji University, Shanghai, China. His current research interests include AI for science, self-rotation in classical wave systems (theory and applications), topological physics (theory and applications), and photonic/phononic crystals.
(Email: longyangphysics@tongji.edu.cn)

Tianchi Ma received the B.E. degree in information engineering from Zhejiang University, Hangzhou, China, in 2024. He is currently pursuing the M.E. degree in electronic and information technology with Zhejiang University, Hangzhou, China. His current research interests include electromagnetic information theory and photonic crystal.
(Email: ma_tianchi@zju.edu.cn)

Jian-Wei Liu received the Ph.D. degree in optics from Sun Yat-sen University, Guangzhou, China, in 2024. He is currently a Post-Doctor at Nanyang Technological University, Singarpore. His current research interests include topological physics and metamaterials.
(Email: jianwei.liu@ntu.edu.sg)

Gui-Geng Liu obtained the B.S. degree in the poling class of physics from Nankai University, Tianjin, China, in 2017 and the Ph.D. degree from Nanyang Technological University, Singapore, in 2023. Then, he continued the postdoctoral research at Nanyang Technological University, Singapore. In 2024, he joined the School of Engineering, Westlake University, Hangzhou, China, as an Assistant Professor (independent PI, doctoral supervisor), and received funding from the National Overseas High-level Talent Youth Program. Dr. Liu has been awarded the Top-Grade Award of National Undergraduate Innovation and Entrepreneurship Training Program in 2017, the Outstanding Undergraduate Thesis in Tianjin in 2017, the Chinese Government Outstanding Self-Financed Student Scholarship in 2021, one of the Top 10 Optical Events with Social Influence in China in 2022, the Gold Medal of Material Research Society of Singapore in Physics in 2023, and the sole Winner of Graduate College Research Excellence Award of Nanyang Technological University in 2023, the Finalist Award of Rising Stars of Light in 2024, and 2024 Forbes China 30 Under 30.
(Email: liuguigeng@westlake.edu.cn)

Yidong Chong received the B.S. degree in physics and the B.S. degree in mathematical and computational sciences from Stanford University, Stanford, CA, USA, in 2003 and the Ph.D. degree from Massachusetts Institute of Technology, Cambridge, MA, USA, in 2008. Since 2024, he has served as a Professor at Nanyang Technological University, Singapore. His current research interests include topological photonics, topological acoustics and electronics, non-Hermitian photonics, and coherent perfect absorbers.
(Email: yidong@ntu.edu.sg)

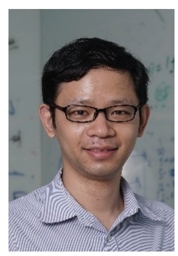

Baile Zhang has been a Professor at the School of Physical and Mathematical Sciences, Nanyang Technological University, Singapore. He received the Ph.D. degree in 2009 from Massachusetts Institute of Technology (MIT), Cambridge, MA, USA, following the B.S. degree in 2003 and the M.S. degree in 2006 from Tsinghua University, Beijing, China, all majored in electrical engineering. Before he joined Nanyang Technological University, Singapore, in 2011, he was a Post-Doctoral Associate at the BioSyM Interdisciplinary Research Group, Singapore-MIT Alliance for Research and Technology Centre, Singapore, and a Visiting Scientist at the 3D Optics Group, Department of Mechanical Engineering, MIT, Cambridge, MA, USA. His research interests included electromagnetic wave theory and applications, metamaterials, optical microscopy, and plasmonic photonics.
(Email: blzhang@ntu.edu.sg)

Er-Ping Li is currently a Qiushi-Distinguished Professor with the Department of Information Science and Electronic Engineering, Zhejiang University, Hangzhou, China. He served as the Founding Dean for the Institute of Zhejiang University-University of Illinois at Urbana-Champaign, Haining, China, in 2016. Since 1993, he has served as a Research Fellow, Associate Professor, Professor, Principal Scientist, and Senior Director at the research institute and university in Singapore. Dr. Li authored or co-authored over 400 papers published in the referred international journals, and also authored two books published by John-Wiley-IEEE Press and Cambridge University Press. He holds and has filed a number of patents at the US patent office. His research interests include electrical modeling and design of micro/nano-scale integrated circuits as well as 3D electronic package integration.
(Email: liep@zju.edu.cn)